Available online at www.sciencedirect.com
ScienceDirect
Catalysis Communications 8 (2007) 1748–1754
CATALYSIS COMMUNICATIONS
www.elsevier.com/locate/catcom

Carbon nanotubes-templated assembly of $LaCoO_3$ nanowires at low temperatures and its excellent catalytic properties for CO oxidation

Fei Teng, Shuhui Liang, Buergen Gaugeu, Ruilong Zong, Wenqing Yao, Yongfa Zhu *

Department of Chemistry, Tsinghua University, Beijing 100084, China

Received 30 October 2006; received in revised form 21 January 2007; accepted 2 February 2007
Available online 12 February 2007

Abstract

This work reports the mild synthesis of $LaCoO_3$ catalyst with the interesting nanowire morphology in the presence of both carbon nanotubes (CNTs) and citrate. In comparison, $LaCoO_3$ nanoparticles were prepared by conventional citrate method. The samples were characterized by TEM (Transmission electron microscopy), XRD (X-ray diffraction), N_2 adsorption isotherm and CO-TPD (Temperature-programming desorption), etc. The results showed that the morphology of $LaCoO_3$ catalyst was controlled effectively by the CNTs template; and that the adding of citrate not only controlled effectively the stoichiometric ratio of La to Co, but also reduced the crystallizing temperature of $LaCoO_3$ crystal greatly. Moreover, after calcined at 750 °C for 48 h, $LaCoO_3$ nanowires exhibited higher thermal stability and catalytic activity for CO oxidation, compared with the nanoparticles.
© 2007 Elsevier B.V. All rights reserved.

Keywords: $LaCoO_3$ nanowires; Carbon nanotubes; Citrate; CO oxidation

1. Introduction

Since the discovery of carbon nanotubes (CNTs) by Iijima in 1991 [1], CNTs have attracted much attention due to their unique mechanical and physical properties [2]. It could expect that CNTs can be employed as template to prepare a new kind of nanostructured materials, which can not be obtained by other synthesis methods. Generally, the wet-chemistry procedures are involved in the CNTs-templated approach, including impregnation, ion exchange, and coprecipitation [3,4]. Ajayan et al. [5], who prepared the uniformed V_2O_5 nanostructures, first reported the CNTs-templated synthesis of oxide/CNTs nanocomposites and oxide fibers. Hereafter, a variety of materials, such as metals, hydroxides, binary oxides and so on [2,6–14], have been fabricated using CNTs as templates. As far as the literatures are concerned, nevertheless, only limited researches have been performed on the CNTs-templated fabrication of ternary metal oxides nanowires, including $MgAl_2O_4$, $CoFe_2O_4$, β-Zeolite, $MnWO_4$ and $CdWO_4$, etc. [14–20].

CO oxidation has important applications in environment protection, such as indoor air cleaning and automotive exhaust treatment, etc. $LaCoO_3$ is one of the most important catalysts for CO oxidation. The prepared $LaCoO_3$ catalysts by conventional methods are usually composed of the nanoparticles, which are easy to sinter at high temperatures. It has been reported that the properties of the catalyst could be improved effectively by controlling its morphology [21]. To the best of our knowledge, nevertheless, the research concerning the CNTs-templated synthesis of $LaCoO_3$ nanowires has been scarcely reported up to now. Due to the difference in the interaction between the different metal components and the CNTs surface, the phase separation is easy to occur upon drying and calcining subsequently. As a result, pure perovskite structure is very difficult to achieve by the CNTs template. Therefore, the synthesis of single-phase $LaCoO_3$ nanowires is still a challenge to researchers. In this article, we report, for the first time, the mild synthesis of $LaCoO_3$ nanowires in the

* Corresponding author. Tel./fax: +86 10 62787601.
E-mail address: zhuyf@mail.tsinghua.edu.cn (Y. Zhu).

1566-7367/$ - see front matter © 2007 Elsevier B.V. All rights reserved.
doi:10.1016/j.catcom.2007.02.005

presence of both carbon nanotubes and citrate. We investigated the morphology control, the low-temperature crystallization, catalytic activity for CO oxidation and thermal stability of $LaCoO_3$ nanowires. In comparison, $LaCoO_3$ nanoparticles were prepared by conventional citrate method.

2. Experimental section

2.1. Materials

Carbon nanotubes (CNTs) were supplied by Department of Chemical Engineering (Tsinghua University), all the other chemicals, including $La(NO_3)_3 \cdot 6H_2O$ (A.R.), $Co(NO_3)_2 \cdot 6H_2O$ (A.R.), Citric acid (CA) ($C_6H_8O_7 \cdot H_2O$, MW = 210, A.R.), were purchased from Beijing Chemicals Company of China and used as received.

2.2. Pretreatment of CNTs

Before use, the original CNTs were treated with concentric HNO_3. Typically, the CNTs (0.5 g) were boiled for 24 h in 100 ml 65 wt% HNO_3 under fluxing; then the CNTs were washed with deionized water and dried in an oven at 80 °C for 24 h. The treatment would purify and functionalize the surface of CNTs due to the generation of oxygen-containing groups by an oxidation process. The amount of introduced the function groups on the surface of CNTs was determined with the well-known Boehm titration method [22]. The concentration of the carboxylate groups (–COOH) on the CNTs was 0.25 mmol mg^{-1}, as determined by adjusting the pH value to 11 using 0.01 M NaOH solution, followed by titration using HCl solution.

2.3. Synthesis of $LaCoO_3$ nanowires

The solution was prepared by dissolving stoichiometric $La(NO_3)_3$, $Co(NO_3)_2$ and citric acid in deionized water, in which the molar ratio of La/Co/CA was kept at 1/1/2. The treated CNTs (0.250 g) were dispersed in the solution above under ultrasonic condition. After sonicating for 30 min, the mixture was stirred magnetically for 24 h. The solids were recovered by centrifuging. After washed with deionized water for 3–4 times, the solids were dried at 80 °C for 24 h; and then the sample was calcined at 600 °C for 5 h in air to remove the CNTs template. To investigate the thermal stability of $LaCoO_3$ catalyst, the sample was further calcined at 750 °C for 48 h in air.

2.4. Characterization

The samples were characterized by X-ray diffraction (XRD) on a Rigaku D/MAX-RB X-ray powder diffractometer, using graphite monochromatized Cu Kα radiation ($\lambda = 0.154$ nm), operating at 40 kV and 50 mA. The patterns were scanned from 10° to 70° (2θ) at a scanning rate of 5° min^{-1}. A nitrogen adsorption isotherm was performed at 77 K on a Micromeritics ASAP2010 gas adsorption analyzer. The sample was degassed at 200 °C for 5 h before the measurement. Surface area and pore size distribution were calculated by BET (Brunauer–Emmett–Teller) and BJH (Barrett–Joyner–Halenda) methods, respectively. The morphology of the catalyst was characterized with a TEM (JEOL 200CX) with the accelerating voltage of 200 kV. The powders were dispersed in ethanol ultrasonically, and then the samples were deposited on a thin amorphous carbon film supported by copper grids. CO-TPD measurements were performed on a conventional CO-TPD instrument. In order to remove the pollutants adsorbed on the catalyst, the catalyst (0.1 g) was loaded in a quartz reactor and heated in He flow at 280 °C for 2 h; under the flowing He gas (40 ml min^{-1}), the system was cooled naturally to room temperature. The sample was then saturated with CO at room temperature for 0.5 h, and the excess of adsorbate was removed by allowing the sample to remain in a He flow until no significant amount of adsorbate can be detected. The temperature ramped to 600 °C at a linear heating rate of 20 °C min^{-1}. Mass spectra (MS) were used to monitor the variations of the m/e ratio of CO (28) to CO_2 (44).

2.5. Evaluation of activity for CO oxidation over the catalysts

The reaction of CO oxidation was carried out in a conventional flow system under atmospheric pressure. Before each catalytic run, the catalyst was flushed with air (100 ml/min) for 1 h at 600 °C, in order to remove adsorbed species at the surface, and then cooled down to 30 °C. Catalyst (0.1 g) was loaded in a quartz reactor (inner diameter: 5 mm), with quartz beads packed at both ends of the catalyst bed. A mixture gas of 2 vol% CO and 98 vol% air was fed into the catalyst bed at a gas hourly space velocity (GHSV) of 12 000 h^{-1}. The compositions of inlet and outlet gases were analyzed by an on-line gas chromatography with a GDX-403 GC-column(1.5 m × 4 mm, 100 °C) and a flame ionization detector (FID).

3. Results and discussion

3.1. Functionalizing and impregnation of CNTs

Fig. 1a and b gives the typical TEM images of CNTs samples before and after treatment with HNO_3, respectively. Fig. 1a reveals that a significant amount of amorphous carbonaceous impurities was contained in the untreated CNTs and the CNTs tangled up or agglomerated severely. After treatment, the impurities were removed completely and the CNTs were almost open (Fig. 1b). The CNTs have the inner diameters in the range of 5–10 nm and the outer diameters in the range of 20–50 nm, with the lengths of up to a few microns.

During the process of the treatment, the oxidation of CNTs by HNO_3 occurred, which gave give rise to a large

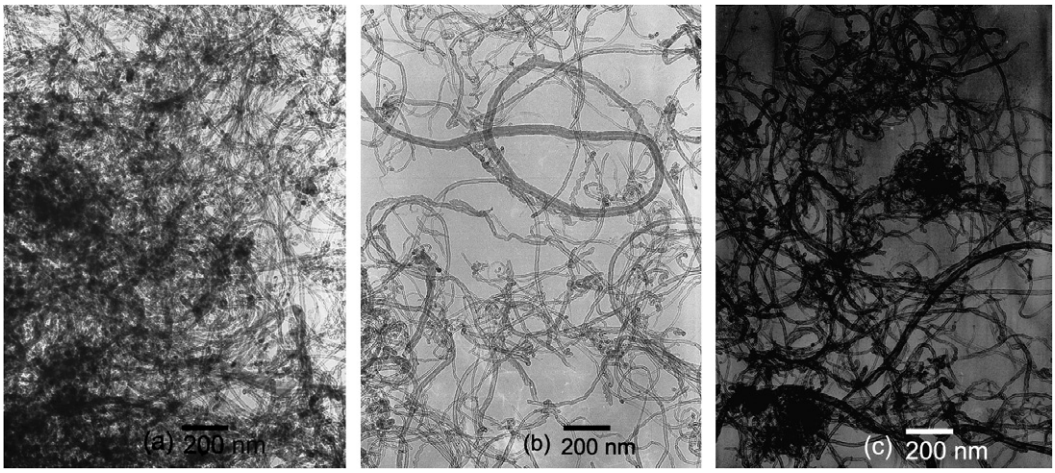

Fig. 1. TEM images of carbon nanotubes (CNTs) and CNTs /nitrates composites: (a) CNTs before treatment; (b) CNTs after treatment; and (c) CNTs/nitrates composites.

amount of oxygen-containing functional groups (hydroxyl and/or carbonyl groups) on the surfaces of CNTs. This has been confirmed by other researchers [22–26]. As a result, the functionalized CNTs can be effectively impregnated with the aqueous solution. Compared with Fig. 1b, the higher contrast of the image indicates that the CNTs have been impregnated with an inorganic phase (Fig. 1c). Although we could not assure, basing on the TEM image, whether the inorganic phase was inside or outside the CNTs, it seems that the coating on the surface and the filling into the CNTs inner might have occurred simultaneously based on the researches [26–30]. Based on the literatures, the effective impregnation resulted from the strong interaction between the inorganic phase and the surface function groups (–COOH and –OH) of CNTs [27]. The oxygen-containing groups on the CNTs surfaces may act as the anchoring sites for the metallic precursors and/or metals. The homogeneous complexes may form through chelating reactions between CNTs-COO– and La/Co [27]. Concerning the filling process, it has been reported that CNTs can be filled satisfactorily by the elements or compounds with a surface tension lower than 200 mN m^{-1} [28–30]. Ugarte et al. reported the inner filling of the open CNTs with molten silver nitrate by capillary forces. They have further demonstrated that only those tubes with inner diameters of 4 nm or more can be filled by the molt salt, suggesting a capillarity size dependence as a result of the lowering of interface energy of the nanotube-salt with increasing curvature of the nanotubes [26]. Therefore, the use of water with a relatively low surface tension (72 m N m^{-1}) as filling solvent can be satisfactorily drawn into the inner cavities of CNTs through capillarity.

Finally, the inorganic phase/CNTs composite was calcined in air in order to remove the template and form the perovskite structure. The results showed that the CNTs were removed completely and the pure perovskite structure was formed at the temperature as low as 600 °C. This is interesting that the temperature is significantly lower than that needed to oxidize the pure CNTs. It is well known that CNTs without any protection can be only oxidized completely to CO_2 in air above 700 °C [31]. The low temperature for CNTs oxidation could be ascribed as to a catalyzing effect of La–Co oxides on the graphitic decomposition, because $LaCoO_3$ is an excellent oxidation catalyst. Eder et al. have also observed the catalyzing effect while they prepared TiO_2 by CNTs [31]. Fig. 2 gives the XRD patterns of the inorganic phase/CNTs composite and $LaCoO_3$ catalyst. After drying at 80 °C, only the diffraction peaks of the carbon template are observed (Fig. 2a); but those originating from the inorganic phases can not be observed, which is probably due to the formation of a homogeneous noncrystalline precursor in the presence of citrate. After calcination at 600 °C for 5 h, the CNTs template has been removed completely and single-phase perovskite was formed (Fig. 2b). All the

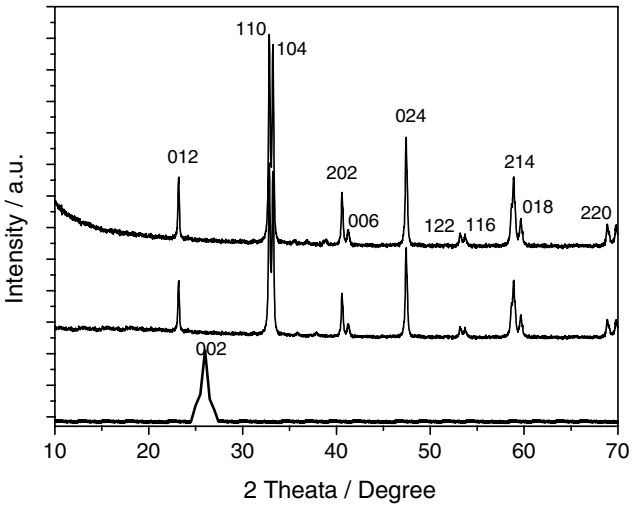

Fig. 2. XRD patterns of the nitrates/CNTs composites and $LaCoO_3$: (a) Nitrates/composites dried at 80 °C; (b) $LaCoO_3$ calcined at 600 °C for 5 h; and (c) $LaCoO_3$ calcined at 750 °C for 48 h.

diffraction peaks can be well indexed to a rhombohedral $LaCoO_3$ (JCPDS 25–1060). The low formation temperature of perovskite structure could be ascribed as to the formation of the homogeneous amorphous precursor in the presence of citric acid [32]. Besides, as far as the formation of perovskite phase deposited on the CNTs is concerned, it could be believe that the nucleation and growth of $LaCoO_3$ crystals were induced and promoted by the solid-state substrate (i.e., the wall of CNTs), basing on the crystallization process from solution [33]. Upon calcining at 750 °C for 48 h, the diffraction peaks of $LaCoO_3$ crystals become sharper, indicating that $LaCoO_3$ crystals have grown to some extent (Fig. 2c).

Further, the morphology of $LaCoO_3$ crystal was observed by TEM, as shown in Fig. 3. After calcined at 600 °C, the resulting $LaCoO_3$ crystals exhibit interesting wire-shaped structures. $LaCoO_3$ nanowires have the diameters in the range of 20–50 nm and the lengths of 1.5–2 μm with an aspect ratio of 50. The morphology of $LaCoO_3$ nanowires truly reflects the templating effect of the CNTs. However, the diameters of $LaCoO_3$ nanowires are much larger than that of the CNTs template, but their lengths are shorter. The possibility is that the neighboring $LaCoO_3$ nanowires coalesced or fused together to form the large ones while calcining. It is clear that the structure of CNTs has a significant influence on the growth of $LaCoO_3$ crystallites. These findings are of specific interest, which could provide us with an insight on how $LaCoO_3$ nanocrystals assembled into $LaCoO_3$ nanowires by the CNTs. Moreover, after calcination at 750 °C for 48 h, $LaCoO_3$ catalyst maintained the wire morphology and a net of nanowires were formed (Fig. 3c). This indicates that $LaCoO_3$ nanowires have a good thermal stability. Nevertheless, it is difficult to obtain the wire-shaped $LaCoO_3$ catalysts by conventional citrate route, but the resulting $LaCoO_3$ catalysts generally consist of the nanoparticles.

3.2. Morphology control and crystallization process of $LaCoO_3$

Note that the roles of the CNTs and citrate in the formation of $LaCoO_3$ nanowires deserve to detail further. Ajayan et al. have reported that a surface-tension effect can induce the growth of uniform thin V_2O_5 films on the outside of nanotubes, along with oxide fillings in the inner cavities of the tubes [5]. As a result, it seems that the CA-metals complex also impregnated the CNTs as the similar way above. The surface properties of the CNTs played a key role in accommodation of the foreign species through a chelating interaction, along with the inner cavities of CNTs as a physical acceptor. While annealing, the inorganic salts decomposed and crystallized to give rise to $LaCoO_3$ nanocrystals. $LaCoO_3$ nanocrystals on the surface of CNTs may grow along the axis parallel to that of the CNTs, the inner nanocrystals also grew along the same axis due to the confining effect by the CNTs. While the CNTs were removed, the intercalation or fusion of the nanocrystals outside and inside the CNTs occurred where the CNTs were missing. Ultimately, the nanowires formed.

The contrast experiment (†see Supporting Information for Fig. S1) showed that without adding citric acid, $LaCoO_3$ crystals were formed at a high temperature (700 °C) and the impurities phases (i.e., $La(OH)_3$ or CoO_x) were always present, although the sample maintained the nanowire morphology. The results indicated that the addition of citric acid not only favored for maintaining the stoichiometric ratio of La to Co, but also reducing the crystallization temperature of perovskite. The formation of $LaCoO_3$ nanowires could be divided into three stages:

(i) Starting chemicals → Homogeneous precursor
(ii) Homogeneous precursor → Nanocrystals
(iii) Nanocrystals → Nanowires

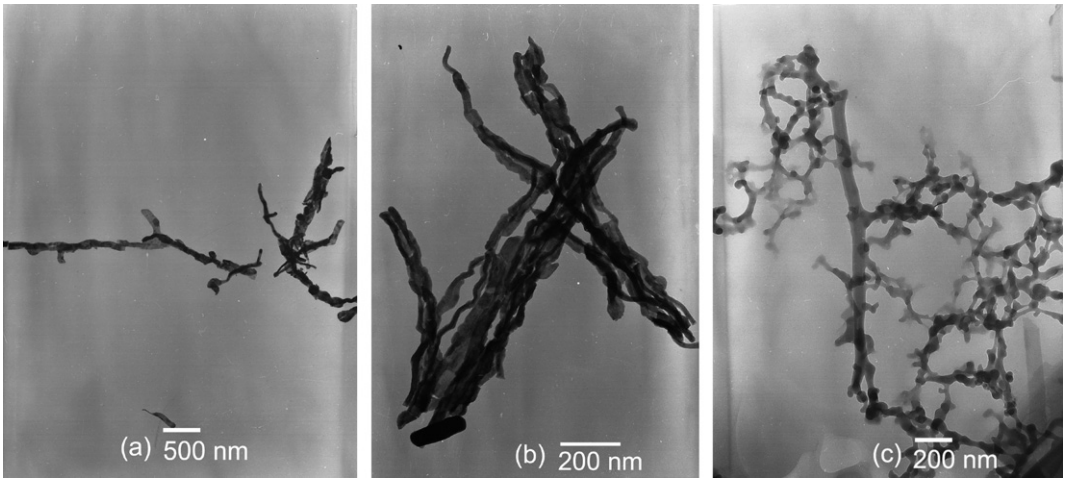

Fig. 3. TEM images of $LaCoO_3$ catalyst: low- (a) and high-magnification; (b) images of $LaCoO_3$ after calcination at 600 °C for 5 h; (c) $LaCoO_3$ after calcination at 750 °C for 48 h.

Due to the strong chelating interaction of citric acid with metals ions, the mixed homogeneity of La and Co in the precursor could be achieved at atomic level, which favors for the subsequent solid-state reaction to form perovskite structure. It has been reported that the perovskite structure can be formed at temperatures as low as 500–600 °C in the presence of citric acid [32,34]. Besides, the formation of perovskite structure may be also promoted by the CNTs. Based on the results by Gogotsi et al. [30], CNTs with an outer diameter of 100 nm can act as miniature pressure vessels and retain pressurized fluid. The macroscopic pressure outside the CNTs remained unchanged, while the inner pressure of increased greatly. The CNTs acted as the nanoreactors that favored for the crystallization of perovskite, similar to a conventional hydrothermal process. Summarily, the conclusions could be drawn as below: (i) the wire morphology of $LaCoO_3$ catalyst can be controlled effectively by the CNTs template; (ii) the adding of citric acid not only controlled the phase composition of perovskite effectively, but also reduced the crystallization temperature of perovskite greatly.

3.3. Catalytic activity for CO oxidation and thermal stability of $LaCoO_3$ nanowires

$LaCoO_3$ is one of the most active oxidation catalyst for CO oxidation, so the catalytic activity of CO oxidation over $LaCoO_3$ nanowires was evaluated. To compare with $LaCoO_3$ nanowires, $LaCoO_3$ nanoparticles were prepared by conventional citrate route (†see Supporting information for Fig. S2). Fig. 4 gives the activities of CO oxidation over $LaCoO_3$ nanowires (designated as S1) and nanoparticles (designated as S2). The complete conversions of CO over S1 and S2 (calcined at 600 °C for 5 h) were achieved at 190 and 170 °C, respectively (dashed lines). Observed from Table 1 and Fig. S2, $LaCoO_3$ nanoparticles of about 40 nm in sizes have higher surface area of 20.5 $m^2\ g^{-1}$, compared with that (14.6 $m^2\ g^{-1}$) of the nanowires, indicating more active sites could be provided by the nanoparticles. Therefore, the catalytic activity of $LaCoO_3$ nanoparticles is higher than that of the nanowires.

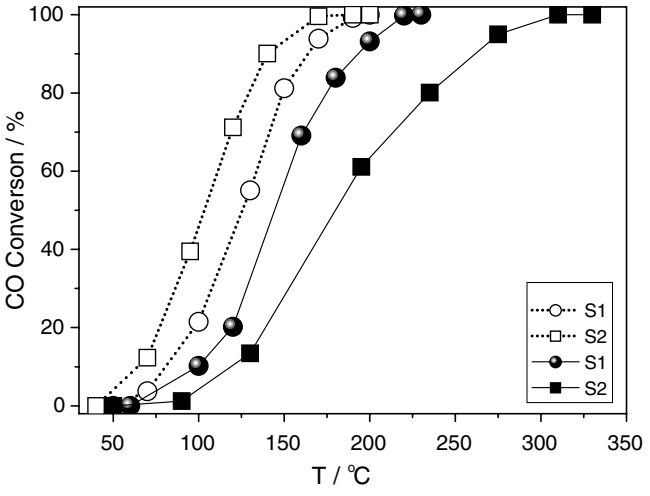

Fig. 4. The activities of CO oxidation over $LaCoO_3$ catalysts: S1, nanowires prepared in the presence of both CNTs and citrate; S2 $LaCoO_3$ nanoparticles prepared via conventional citrate route, Dashed and solid lines, after calcination at 600 °C for 5 h and 750 °C for 48 h, respectively.

However, the thermal stability of catalyst is also a very important factor for practical applications. In order to investigate the thermal stabilities of the catalysts, $LaCoO_3$ nanowires and nanoparticles were further calcined at a high temperature for a long duration. Even after calcination at 750 °C for 48 h, the surface area of $LaCoO_3$ nanowires decreased slightly to 13.9 $m^2\ g^{-1}$. As a result, the complete conversion temperature of CO over $LaCoO_3$ nanowires reached 220 °C. After calcination at 750 °C for 48 h, however, $LaCoO_3$ nanoparticles sintered severely, and the catalyst size increased significantly from 40 to 100 nm and more (†see Supporting information for Fig. S2), resulting in the significant decrease of surface area (20.5 vs. 12.1 $m^2\ g^{-1}$). As a result, the catalytic activity for CO complete oxidation over the nanoparticles decreased steeply (310 °C). It is clear that $LaCoO_3$ nanowires had higher thermal stability than the nanoparticles. Considering their same crystal structures, the high thermal stability of the nanowires could be closely related to the unique one-dimensional morphology. It is generally accepted that the sintering and nucleation of crystals occur initially at the contacting points among the particles [35,36]. The nanoparticles are apt to pack closely, meaning that there would be more contacting points among them; however, the nanowires have the tendency to form a loose structure, in which the contacting points among the nanowires are less. Indeed, observed from Table 1, the nanowires have larger pore volume and pore size (0.26 ml g^{-1}, 15.7 nm) than those (0.09 ml g^{-1}, 7.7 nm) of the nanoparticles. The decrease of contacting chance would suppress the sintering to some extent. As a result, $LaCoO_3$ nanoparticles would sinter more severely than the nanowires upon long-duration calcination. Teng and Barry et al. have previously prepared fibrous Al_2O_3 with high surface areas at high temperatures. They also attributed the high ability resistant to sintering to the crude structure and fiberform morphology of Al_2O_3 particles [37,38].

Table 1
The textural properties of $LaCoO_3$ catalysts with different morphologies

Sample	Preparation	SA[b] ($m^2\ g^{-1}$)	V_{pore}[b] (ml g^{-1})	d_{pore}[b] (nm)
S1[a]	600 °C, 5 h	14.6	0.20	15.7
	750 °C, 48 h	13.9	0.18	9.5
S2[a]	600 °C, 5 h	20.5	0.09	7.7
	750 °C, 48 h	12.1	0.05	2.4

[a] S1, $LaCoO_3$ nanowires by coupling CNTs with citrate; S2, $LaCoO_3$ nanoparticles by citrate route.

[b] SA, Surface area by BET method, V_{pore}, adsorption volume, d_{pore}, average pore size by BJH method.

Concerning catalytic mechanism, the catalytic oxidation of CO has been considered as the so-called suprafacial catalytic process [39], in which the crystal structure and the surface properties of the catalyst seem to be very important. Tascon et al. proposed the following catalytic mechanism of CO oxidation on $LaCoO_3$ [40]:

$$O_2(g) \rightarrow O_2(ads) \rightarrow 2O(ads)$$

$$CO(g) \rightarrow CO(ads)$$

$$CO(ads) + 2O(ads) \rightarrow CO_3(ads)$$

$$CO_3(ads) \rightarrow CO_2(ads) + O(ads)$$

$$CO_2(ads) \rightarrow CO_2(g)$$

The authors suggested that cobalt and oxygen sites act as adsorption and activation centers for CO and O_2, respectively. Similar to that over $LnSrNiO_4$, the adsorbed CO on cobalt site reacts with the lattice oxygen, whereas the chemisorbed oxygen transforms into the lattice oxygen to reinforce the consumed lattice oxygen [41]. It has been proposed that the oxygen transformation occurs in CoO_6 octahedral [42], and cobalt site is the active center for CO and the lattice oxygen is active oxygen species. Therefore, the adsorption of reactants on the catalyst played in an important role in CO oxidation. CO-TPD (Temperature-Programmed Desorption) was performed to explore CO adsorption on $LaCoO_3$ catalysts, as shown in Fig. 5. A significant portion of CO desorbed as a form of CO_2 in the process, so the total adsorption amount of CO on the catalyst was consistent with the desorption amounts of both CO_2 and CO. For $LaCoO_3$ nanowires, six desorption peaks (70,150, 280, 340, 430 and 560 °C) of CO_2 are observed; but only three peaks (370, 430, 560 °C) are observed for $LaCoO_3$ particles (Fig. 5a). Observed from Fig. 5b, four desorption peaks of CO (160, 330, 360, 550 °C) are observed for $LaCoO_3$ nanowires, but only two peaks (430, 510 °C) are observed for the nanoparticles. It is clear that the intensities of CO_2 (CO) desorption peaks over the nanowires are higher than those of the particles. The quantitative analysis results showed that the total adsorption amount of CO on $LaCoO_3$ nanowires is larger than that on the particles, indicating that there may be more active centers on $LaCoO_3$ nanowires than those on the latter. The results agree well with the activity order of CO oxidation over the $LaCoO_3$ catalysts after calcination at 750 °C for 48 h.

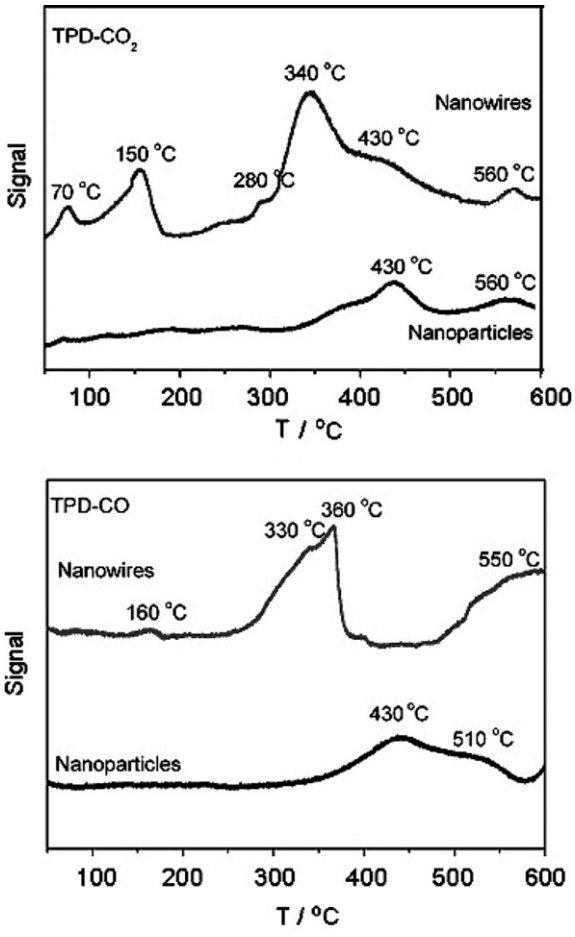

Fig. 5. CO_2-TPD and CO-TPD profiles of CO adsorption on $LaCoO_3$ catalysts calcined at 750 °C for 48 h.

4. Conclusions

In the presence of both CNTs and citrate, $LaCoO_3$ nanowires can be prepared at the temperature as low as 600 °C. Both CNTs and citrate played the important roles in the formation of the single-phase $LaCoO_3$ nanowires. Moreover, after calcinations at 750 °C for 48 h, $LaCoO_3$ nanowires showed higher thermal stability and activity of CO oxidation, compared with the nanoparticle counterpart. CNTs as removable templates could lead to useful new kinds of nanostructured materials.

Acknowledgements

This work is supported by Chinese National Science Foundation (Nos. 20433010, 20571047). We are grateful to Dr. Yu Fan of China University of Petroleum (Beijing) for the TPD-CO data.

Appendix A. Supplementary data

TEM images and XRD patterns of $LaCoO_3$ samples prepared by CNTs without adding citric acid and by conventional citrate route. This material is available free of charge via the Internet at www.elsevier.com. Supplementary data associated with this article can be found, in the online version, at doi:10.1016/j.catcom.2007.02.005.

References

[1] S. Iijima, Nature 354 (1991) 56.
[2] R.L.D. Whitby, W.K. Hsu, Y.Q. Zhu, H.W. Kroto, D.R.M. Walton, Phil. Trans. R. Soc. Lond. A 362 (2004) 2127.
[3] K. Koga, G.T. Gao, H. Tanaka, X.C. Zeng, Nature 412 (2001) 802.
[4] M.S.P. Sansom, P.C. Biggin, Nature 414 (2001) 156.

[5] P.M. Ajayan, O. Stephan, P. Redlich, C. Colliex, Nature 375 (1995) 564.
[6] T.M. Day, P.R. Unwin, N.R. Wilson, J.V. Macpherson, J. Am. Chem. Soc. 127 (2005) 10639.
[7] S. Fullam, D. Cottell, H. Rensmo, D. Fitzmaurice, Adv. Mater. 12 (19) (2000) 1430.
[8] M.A. Correa-Duarte, J. Pérez-Juste, A. Sánchez-Iglesias, M. Giersig, L.M. Liz-Marzán, Angew. Chem., Int. Ed. 44 (2005) 4375.
[9] V.P. Dravid, Nature 374 (1995) 602.
[10] W.Q. Han, A. Zettl, NanoLetter 3 (2003) 681.
[11] C.N.R. Rao, B.C. Satishkumar, A. Govindaraj, Chem. Commun. 16 (1997) 1581.
[12] S. Banerjee, S.S. Wong, NanoLetter 2 (2002) 195.
[13] B.C. Satishkumar, A. Govindaraj, M. Nath, C.N.R. Rao, J. Mater. Chem. 10 (2000) 2115.
[14] G.R. Patzke, F. Krumeich, R. Nesper, Angew. Chem., Int. Ed. 41 (2002) 2446.
[15] E. Flahaut, A. Peigney, C. Laurent, C. Marliere, F. Chastel, A. Rousset, Acta Mater. 48 (2000) 3803.
[16] C. Pham-Huu, N. Keller, C. Estournes, G. Ehret, M.J. Ledoux, Chem. Commun. 1 (2002) 1882.
[17] N. Keller, C. Pham-Huu, T. Shiga, C. Estournés, J.-M. Grenéche, M.J. Ledoux, J. Magn. Magn. Mater. 272 (2004) 1642.
[18] M.A. Camblor, A. Corma, S. Valencia, Micropor. Mesopor. Mater. 25 (1998) 59.
[19] C.J.H. Jacobsen, C. Madsen, T.V.W. Janssens, H.J. Jakobsen, J. Skibsted, Micropor. Mesopor. Mater. 39 (2000) 393.
[20] S. Hirano, K. Kato, J. Non-Cryst. Solids 100 (1988) 538.
[21] S.S. Wong, A.T. Woolley, E. Joselevich, C.L. Cheung, C.M. Lieber, J. Am. Chem. Soc. 120 (1998) 8557.
[22] H.P. Boehm, E. Diehl, W. Heck, R. Sappok, Angew. Chem. 76 (1964) 742.
[23] L. Liu, Y. Qin, Z.-X. Guo, D. Zhu, Carbon 41 (2003) 331.
[24] R.M. Lago, S.C. Tsang, K.L. Lu, Y.K. Chen, M.L.H. Green, J. Chem. Soc., Chem. Commun. 13 (1995) 1355.
[25] H. Hiura, T.W. Ebbesen, K. Tanigaki, Adv. Mater. 7 (3) (1995) 275.
[26] T.W. Ebbesen, P.M. Ajayan, H. Hiura, K. Tanigaki, Nature 367 (1994) 519.
[27] D. Ugarte, A. Chatelain, W.A. deHeer, Science 274 (1996) 1897.
[28] E. Dujardin, T.W. Ebbesen, H. Hiura, K. Tanigaki, Science 265 (1994) 1850.
[29] P.M. Ajayan, T.W. Ebbesen, T. Ichihashi, S. Iijima, K. Tanigraki, H. Hlura, Nature 362 (1993) 522.
[30] Y. Gogotsi, J.A. Libera, A.G. Yazicioglu, C.M. Megaridis, in: Nanotubes and Related Materials, Materials Research Society Symposium Proceedings, vol. 633, Pittsburgh, Pennsylvania, 2001, pp. A7.4.1.
[31] D. Eder, I.A. Kinloch, A.H. Windle, Chem. Commun. 13 (2006) 1448.
[32] S. Bilger, E. Syskakis, A. Naoumidia, H. Nickel, J. Am. Ceram. Soc. 75 (1992) 964.
[33] I. Maurin, P. Barboux, J.P. Boilot, Mater. Res. Symp. Ser. 453 (1997) 41.
[34] W.D. Yang, Y.H. Chang, S.H. Huang, J. Eur. Ceram. Soc. 25 (16) (2005) 3611.
[35] T. Horiuchi, T. Osaki, T. Sugiyama, T. Mori, J. Non-Cryst. Solids 291 (2001) 187.
[36] T. Ishikawa, R. Ohashi, H. Nakabayashi, A. Ueno, A. Furuta, J. Catal. 134 (1992) 87.
[37] H. Zhu, J.D. Riches, J.C. Barry, Chem. Mater. 14 (2002) 2086.
[38] F. Teng, J. Wang, Z. Tian, G. Xiong, L. Lin, Mater. Sci. Eng. B 116 (2005) 215.
[39] R.J.H. Voorhoeve, J.P. Remeika, L.E. Tribble, Ann. NY Acad. Sci. 272 (1976) 3.
[40] J.M.D. Tascon, J.L.G. Fierro, L.G. Tejuca, Phys. Chem. 124 (1981) 249.
[41] H. Lou, H. Zhen, J. Yang, Z. Yao, S. Yu, F. Ma, Chem. J. Chin. Univ. 16 (1995) 107.
[42] X. Yang, L. Luo, H. Zhong, Appl. Catal. A–Gen. 272 (2004) 299.